ES Materials & Manufacturing

RESEARCH PAPER View Article Online

A Facile Synthesis of Ag/TiO_2/rGO Nanocomposites with Enhanced Visible Light Photocatalytic Activity

Meiyan Yu[1], Teng Yu[1], Shougang Chen[1*], Zhanhu Guo[2] and Ilwoo Seok[3*]

Ag/TiO_2/rGO (silver/titanium-dioxide/reduced graphene oxide) photocatalysts were synthesized by a facile method that without using any inorganic or organic reducing agents. In this research, supercritical water was used as green reducing agent under the hydrothermal condition. The performance and characterization of nanocomposite materials were verified by various measurements: TEM, FTIR, XPS and DRS. Compared with pure TiO_2 and TiO_2/rGO, newly synthesized material of Ag/TiO_2/rGO photocatalyst performed a significantly increased absorption in the range of visible light and improved photocatalytic activity. The interaction between anatase nanoparticles and rGO sheets partially contributed to this result due to the surface plasmon resonance (SPR) of silver nanoparticles. This work gives a promising methodology for new materials to develop a new TiO_2-based photocatalyst with high solar absorption and enhanced catalytic activity.

Keywords: Ag /TiO_2/rGO; Nanocomposite; Supercritical water; Photocatalytic activity

Received 15 February 2020, **Accepted** 1 March 2020

DOI: 10.30919/esmm5f712

1. Introduction

As an excellent semiconductor photocatalyst, titanium dioxide (TiO_2) has been extensively applied to solve many of environmental problems that include the photocatalytic degradation of organic contaminants in wastewater or air. TiO_2 has significant properties of high chemical stability, powerful catalytic activity, potent oxidative ability, and nontoxicity. However, despite of best material of photocatalysts, TiO_2 has its own inherent defects. Primarily, its wide band gap with 3.0-3.2 eV limits the absorption of solar spectrum. Besides, its low level of quantum yields because of easy recombination to photogenerated electrons and holes leads to the low photocatalytic efficiency. [1-3] All these defects obstruct the widespread application of TiO_2. For this reason, various strategies have been investigated to overcome these disadvantages by means of doping with nonmetal elements,[4-6] coupling with other semiconductors, [7,8] and loading noble metals.[1,9]

Graphene, a two-dimensional carbon material with excellent properties with high electric charge carrier mobility, intrinsic large surface to volume ratio, capability of chemical functionalization and mechanical flexibility,[10-12] has offered an exciting opportunity to fabricate photocatalytic nanocomposites to obtain desirable performances. As a photocatalyst material, graphene enhanced the absorptivity of photocatalyst, decreased the electron-hole recombination rate due to its high electric charge mobility, and extended π-π conjugation structure with large surface area. This caused the development of TiO_2-graphene composite materials for the improved photocatalytic activity.[13-15]

Moreover, noble metal nanoparticles (NPs) such as Ag or Au also have been applied to improve the photocatalysis properties of TiO_2. The use of NPs has a benefit to reduce the recombination of electron-pole pairs by transferring photogenerated-electrons onto themselves. In addition, Ag or Au NPs absorb the visible light because of the localized

[1] *College of Materials Science and Engineering, Ocean University of China, Qingdao, 266100, China*
[2] *Department of Chemical and Biomolecular Engineering, University of Tennessee, Knoxville, TN 37996, USA*
[3] *College of Engineering and Computer Sciences, Arkansas State University, State University , AR 72467, USA*
***E-mail:** iseok@astate.edu（I. Seok）; sgchen@ouc.edu.cn (S. G. Chen)*

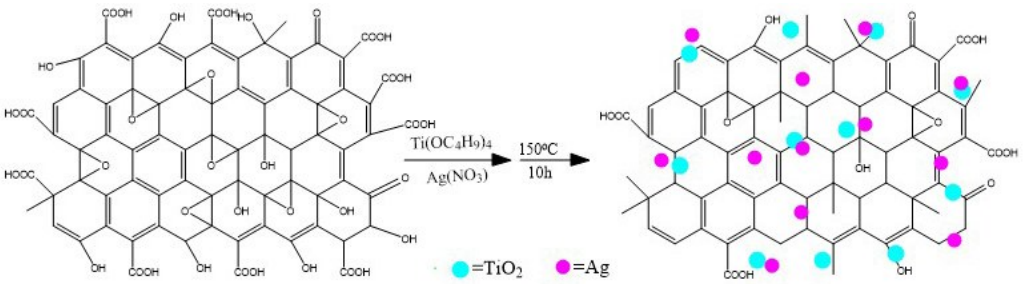

Fig. 1 Synthesis process of Ag/ TiO_2 /rGO nanocomposites.

surface plasmon resonance (LSPR)[16-18] that expands pure TiO_2's absorption to visible range of light. During the past few years, several researches have been reported about the effect of Ag/TiO_2/graphene oxide (GO) on toxic and harsh reducing agents such as dimethylacetamide, hydrazine or sodium borohydride. [19,20] Compared with graphene oxide (GO), the reduced graphene oxide (rGO) is necessary to improve the charge shuttling and possible catalytic position.

In this research, Ag/TiO_2/rGO nano-photocatalyst had been synthesized by a facile method without any inorganic or organic reducing agents. Supercritical water was used as a green reducing agent under the hydrothermal condition. The photocatalytic performance of the prepared nanocomposites was evaluated by the degradation of methylene blue under the visible-light. The materials structures and compositions were characterized with various methods of X-ray powder diffraction (XRD), transmission electron microscope (TEM), selective area electron diffraction (SAED), X-ray photoelectron spectroscopy (XPS) and Fourier-transform infrared spectroscopy (FT-IR). The photocatalytic performance was then measured by ultraviolet-visible (UV-VIS) and diffuse reflectance absorption (DRS) spectroscopy analysis.

2. Experimental Section

2.1 Synthesis of Ag/TiO_2/rGO Nanocomposite

Tetrabutyl titanate (Analytic Reagent (A.R) 99.0%) and Silver nitrate (A. R. ⩾ 99.8%) were obtained from Sinopharm Chemical Reagent Co., Ltd. Graphite materials were purchased from Sigma Aldrich. And graphene oxide (GO) was prepared using a modified Hummers method[21] and then dispersed into the deionized water under ultrasonic condition for 30 min.

Ag/TiO_2/rGO was prepared by a facile hydrothermal method without using any of toxic and harsh reducing agents. The synthesis process was depicted in Fig. 1. Firstly, 5 ml $Ti(OC_4H_9)_4$ and 0.018 g Sodium dodecyl sulfate (SDS) were dissolved into 12 ml ethanol, stirring 30 min, then solution A was obtained. For solution B, 0.024 g $AgNO_3$ was dissolved into 25 ml ethanol, and 0.03 ml HNO_3 (68%) and 0.5 ml deionized water were added. Solution C was prepared by dropping B into the solution A. This solution C was dropped into 50 ml GO solution (0.5 mg mL^{-1}) and stirred 3 hours sequentially until homogeneously distributed. Such mixed solution was placed into a teflon stainless autoclave and heated 150 °C for 10 h. Finally, the mixture was washed several times with deionized water and ethanol, filtered, and dried in an oven at 60 °C.

2.2 Characterizations

X-ray powder diffraction (XRD) patterns of Ag/TiO_2/rGO nanocomposites were obtained on an X-ray diffractometer (Bruker instrument, D8 Advance, Germany) with Ni filtered Cu K (alpha) radiation. The Fourier-transform infrared spectroscopy (FT-IR) measurement was carried out on a Nicolet FTIR 760 infrared spectrometer using Potassium bromide (KBr) pellets. The morphology of nanocrystals and selective area electron diffraction (SAED) patterns was observed with H-7650 transmission electron microscope (TEM, Hitachi, Japan). X-ray photoelectron spectroscopy (XPS) measurement was conducted on X-ray photoelectron spectrometer (Thermo ESCALAB 250Xi, American) with Al K (alpha) radiation. Diffuse reflectance absorption spectra and ultraviolet-visible (UV-VIS) spectra were recorded on a U-3900H UV-VIS DRS spectrophotometer (Hitachi, Japan), and barium sulfate ($BaSO_4$) was used as the reference.

2.3 Photodegradation Experiment

The photocatalytic degradation of methylene blue (MB) was performed at ambient temperature. The design of photochemical reactor was described in Fig. 2. 20 mg catalyst was dispersed into 100 mL of 10 mg/mL MB solution under ultrasonication for 30 min. Before illumination, the mixed system was stirred in the dark for 1 hour to establish adsorption-desorption equilibrium and then exposed to the visible light using the light source of 150 W Xenon (Xe) lamp. At given intervals, 5 mL of suspension was taken, centrifuged, and filtrated to remove the catalyst. The supernatant was used to determine the concentration by measuring the absorbance of MB (λ = 664 nm).

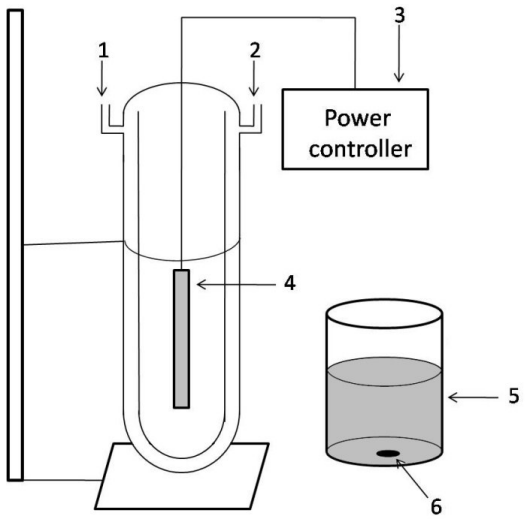

Fig. 2 Schematic diagram of photochemical reactor: (1) cooling water inlet, (2) cooling water outlet, (3) power controller, (4) UV lamp, (5) MB solution and photocatalyst, and (6) Stirring magnet.

3. Results and Discussion

3.1 Characterization of Ag/TiO_2/rGO Nanocomposite

The morphology of pure TiO_2 nano-powder was imaged by TEM as shown in Fig. 3 (left). The size is about 17 nm with an obvious agglomeration. Fig. 3 (right) indicates that graphene is a sheet with several layers and small wrinkles. Some spherical or oval nanocrystals with the size of about 10 nm are randomly distributed on the graphene sheets. The selected area electron diffraction (SAED) patterns of Fig. 4 verify the existence of TiO_2 and Ag. Fig. 4 (right) corresponds to the anatase diffraction planes of (101), (004) and (200). Fig. 4 (right) shows the (111), (311) and (222) crystal planes of face centered cubic (FCC) of Ag.

Fig. 5 shows the result of the XRD patterns of the samples. The peaks at 2θ values of 25.3°, 37.8°, 48.0°, 53.9°, 55.0°, 62.8° and 68.8° can be aligned along to the anatase (JCPDS NO. 021-1272)- corresponding to (101), (004), (202), (105), (211), and (204) planes, respectively. However, a peak at 25° for graphene is absent, which should be overlapped by the strong peak of anatase (101) at 25.3°. In addition, the peak of GO at 12.6° is not observed because the amount of GO has been reduced and transformed to the graphene under our hydrothermal conditions. The peaks belonging to metallic Ag are not observed either in SAED patterns as shown in Fig. 4, which possibly due to the remarkably less and little of Ag particles.[22]

The FT-IR spectra of the samples are shown in Fig. 6. A peak at 3410 cm^{-1} is assigned to stretching vibrational modes of hydroxyl groups on the graphene and TiO_2 surface. The peak at 1650 cm^{-1} can be marked to the C-C vibrational modes of

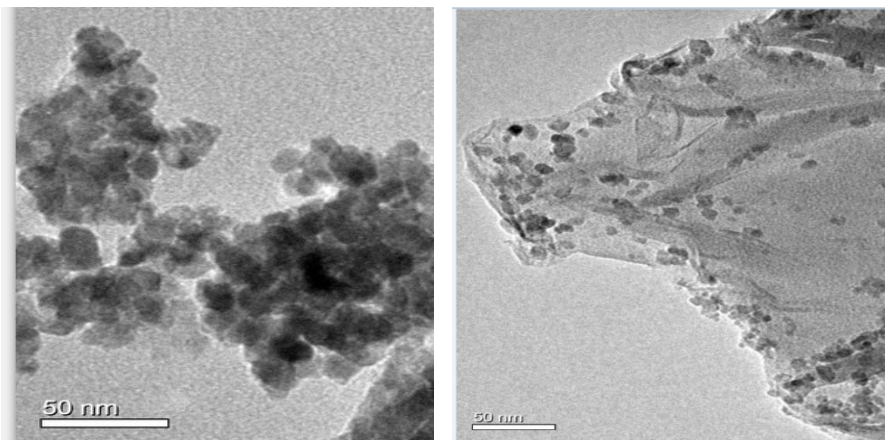

Fig. 3 TEM images of products TiO_2 (left) and Ag/TiO_2/rGO (right).

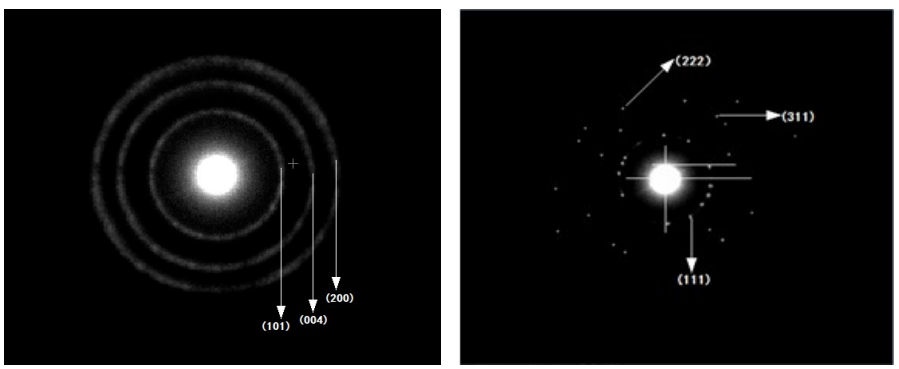

Fig. 4 SAED patterns image of TiO_2 (left) and Ag (right).

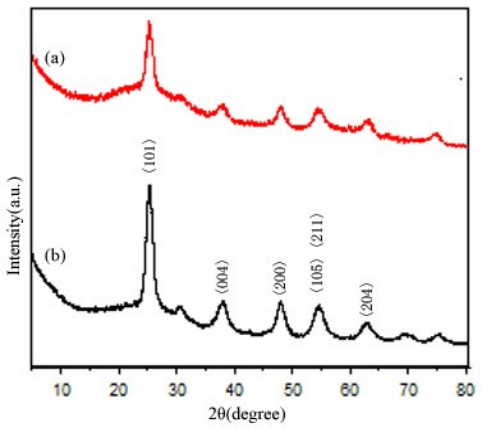

Fig. 5 XRD patterns of (a) $Ag/TiO_2/rGO$ and (b) TiO_2/rGO.

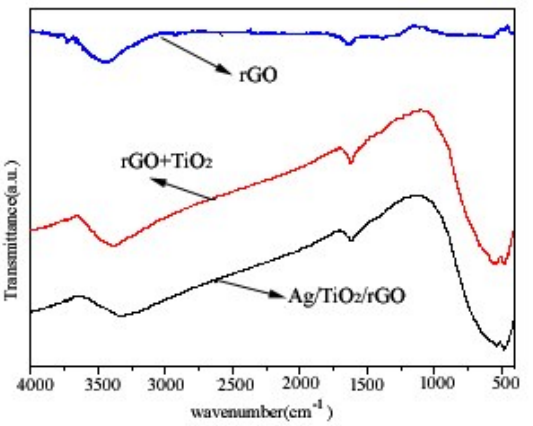

Fig. 6 FT-IR spectra of TiO_2/rGO, $Ag/TiO_2/rGO$, and rGO.

graphene sheets. It is worth noting that the characteristic peak of C=O group is not obvious in Fig. 6, which proves the successful reduction of GO to rGO after hydrothermal process.[23] In addition, a strong and broad adsorption peak over the range of 500-1000 cm^{-1} is observed in the spectra of TiO_2/rGO and $Ag/TiO_2/rGO$. The broadening peak is attributed to the formation of Ti-C-O bonds (~798 cm^{-1}) which overlaps with the bending and stretching vibrational modes of Ti-O-Ti bonds (~670 and 571 cm^{-1}).[24] The existence of Ti-O-C bonds confirms that the formation of chemical bonds between graphene and TiO_2 nanostructures exist.

Diffuse reflectance spectroscopy (DRS) is performed to evaluate the optical performance of $Ag/TiO_2/rGO$ nanocomposite. It is widely recognized that the absorption ability of the photocatalyst **plays** an important role in the photocatalysis process. Fig. 7(a) shows the DRS results of $Ag/TiO_2/rGO$, TiO_2/rGO, and pure TiO_2. It is obvious that not only a red shift occurs in absorption, but also a light absorption between 400 and 800 nm is increased when the sheets of rGO and Ag nanoparticles are used to form the $Ag/TiO_2/rGO$ nanocomposite. On the one hand, The interaction between anatase nanoparticles and rGO sheets partially contributed to this result due to the strong surface plasmon resonance (SPR) absorption of Ag nanoparticles.[25,26] Fig. 7 (b) shows the plot of transformed Kubelka-Munk function versus the energy of light. The band gaps are 3.15 eV, 2.5 eV, and 2.3 eV, for the pure TiO_2, TiO_2/rGO, and $Ag/TiO_2/rGO$, respectively. This variation leads to the absorption edge of $Ag/TiO_2/rGO$ extending into the visible light region. Therefore, the ternary composite is expected to improve the photocatalytic activity, which will be proved in the photocatalytic degradation process of methylene blue (MB) dye.

The corresponding XPS spectra provide further structural information for the $Ag/TiO_2/rGO$ nanocomposite. Fig. 8(a) shows the full-scale spectrum of $Ag/TiO_2/rGO$. It can be seen that the Ti, C, Ag and O elements co-exist. The binding energy at 284.7, 368.3, 459.4, 530.3 and 582.4 eV correspond to the C1s, Ag3d, Ti2p, O1s and Ti2s, respectively. Fig. 8(b) shows the C1s XPS spectrum of $Ag/TiO_2/rGO$ nanocomposite. The peaks at 284.5, 285.3, 286.7 and 288.5 eV are corresponded to the C-C, C-OH, C-O and C=O, respectively.[29] In Fig. 8(c), the peaks at 367.8 and 373.9 eV can be attributed to $Ag3d_{5/2}$ and $Ag3d_{3/2}$ binding energy,[27] which proved the reduction of Ag^+ to

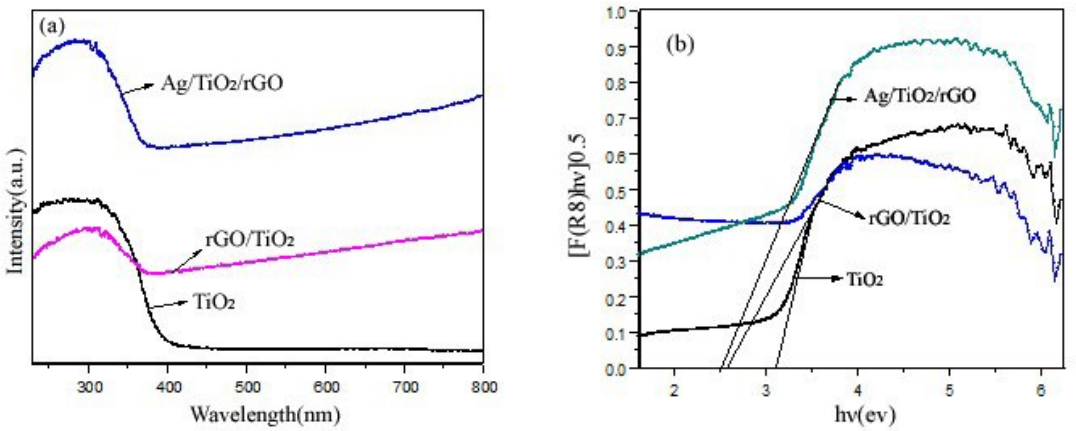

Fig. 7 (a) Diffuse reflectance spectra of $Ag/TiO_2/rGO$, TiO_2/rGO and pure TiO_2; (b) The plot of transformed Kubelka-Munk function versus the energy of light of $Ag/TiO_2/rGO$, TiO_2/rGO and pure TiO_2.

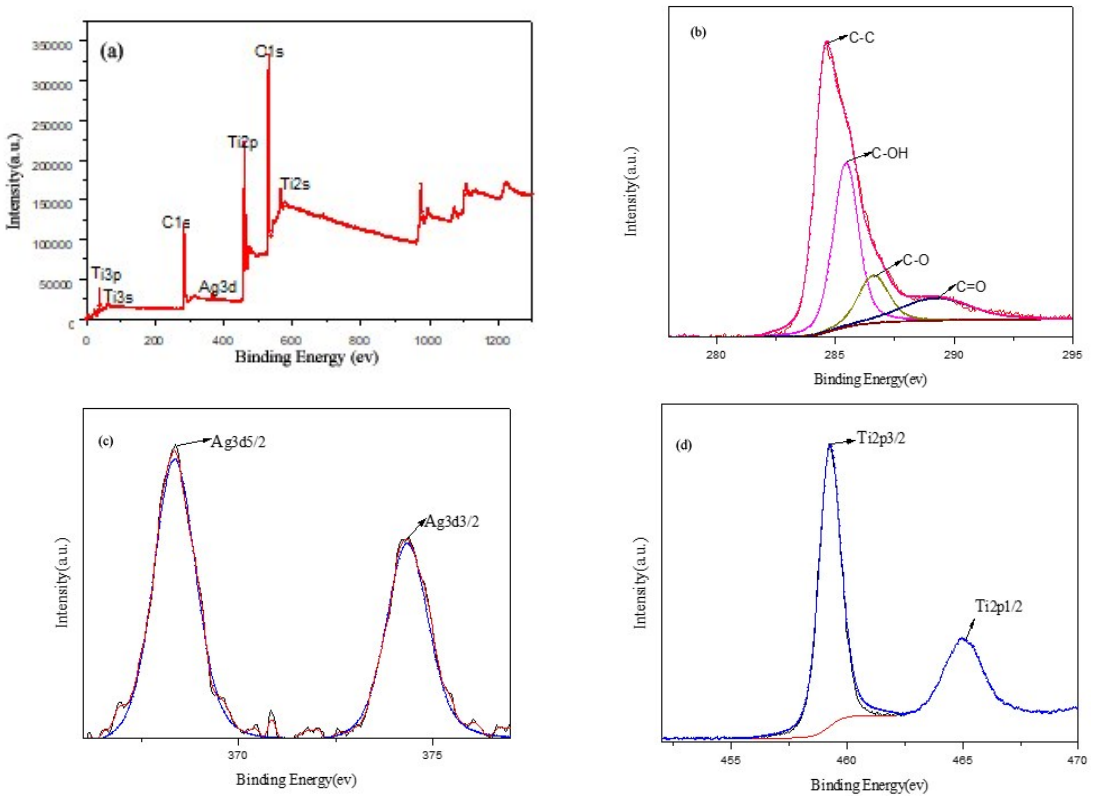

Fig. 8 XPS spectrum of (a) Ag/TiO_2/rGO, (b) C1s, (c) Ag3d, and (d) Ti2p.

metallic Ag nanoparticles. Fig. 8(d), two peaks at 459.1 and 465.0 ev observed in the Ti2p XPS spectrum can be assigned to $Ti2p_{3/2}$ and $Ti2p_{1/2}$,[28] respectively.

3.2 Photocatalytic Activity of Ag/ TiO_2/rGO Nanocomposite

The photocatalytic activity of Ag/TiO_2/rGO nanocomposite was measured by the photocatalytic degradation process of methylene blue dye under visible light of Xe lamp ($\lambda > 400$ nm). Before illumination,the mixed system was stirred in the dark for 1 h to maintain adsorption-desorption equilibrium. Fig. 9 shows the degradation results of pure TiO_2, TiO_2/rGO and Ag/TiO_2/rGO. The adsorption of TiO_2/rGO and Ag/TiO_2/rGO is stronger than pure TiO_2 in the dark. Two major factors may cause this. One is the π-π conjugation between MB and the graphene with intrinsic large surface area. The other is the effect of TiO_2 nanoparticles that keeps the graphene sheets aggregating themselves. In addition, the photocatalytic activity of TiO_2/rGO and Ag/TiO_2/rGO is higher than pure TiO_2, which can be attributed to the significantly enhanced electron-hole pairs separation with the electron injection into graphene to prohibit the photogenerated electron-hole pairs recombination.[5] In comparison between TiO_2/rGO with Ag/TiO_2/rGO, the existence of Ag nanoparticles improved the photocatalytic ability of ternary nanocomposite. It is the effect of the presence of Schottky barriers at the interface of Ag and TiO_2 which served as an electron trap to prevent electron-pole

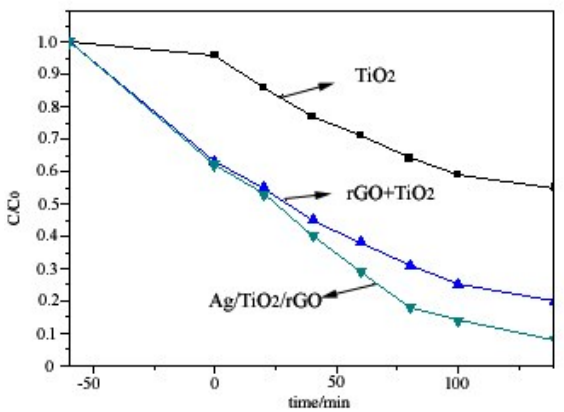

Fig. 9 Photocatalytic degradation of methylene blue for pure TiO_2, TiO_2/rGO and Ag/TiO_2/rGO.

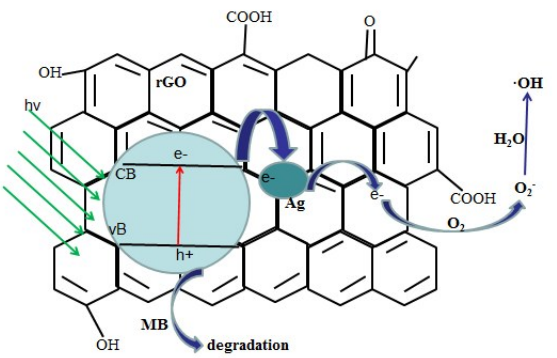

Fig. 10 Pathways of electron transfer and degradation mechanism of MB dye.

recombination.[29,30] Fig. 10 shows the pathways of electron transfer and mechanism of the degradation of MB dye.

4. Conclusions

Without using any inorganic or organic reducing agents, Ag/TiO_2/rGO nano photocatalyst was successfully synthesized under the hydrothermal condition. The nanocomposite was characterized by different experimental measurements. The photocatalytic performance of the nanocomposite was evaluated by the degradation of methylene blue under the visible-light. The results show that the photocatalytic activity of TiO_2 was substantially improved by using graphene and Ag materials. This work gives a promising methodology for new materials to develop a new TiO_2-based photocatalyst with high solar absorption and enhanced catalytic activity.

Conflicts of Interest

All of authors do not have any conflicts to declare.

Acknowledgements

This work was supported by the National Natural Science Foundation (51572249) and the National Natural Science Foundation (51302254).

References

1. H. Liang, B. Zhang, H. Ge, X. Gu, S. Zhang and Y. Qin, *ACS Catal*., 2017, **7**, 6567-6572.
2. L. Ren, Y. Li, J. Hou, X. Zhao and C. Pan, *ACS Appl. Mater. Interfaces*, 2014, **6**, 1608-1615.
3. L. Sun, Z. Zhao, Y. Zhou and L. Liu, *Nanoscale*, 2012, **4**, 613-620.
4. X. Chen and S. S. Mao, *Chem. Rev.*, 2007, **107**, 2891-2959.
5. X. Pan, Y. Zhao, S. Liu, C. L. Korzeniewski, S. Wang and Z. Fan, *ACS Appl. Mater. Interfaces*, 2012, **4**, 3944-3950.
6. M. Zeng, Y. Li, M. Mao, J. Bai, L. Ren and X. Zhao, *ACS Catal.*, 2015, **5**, 3278-3286.
7. X. Chen, L. Liu, P. Y. Yu and S. S. Mao, *Science,* 2011, **331**, 746.
8. J. Kim, S. Choi, J. Noh, S. Yoon, S. Lee, T. Noh, A. J. Frank and K. Hong, *Langmuir,* 2009, **25**, 5348-5351.
9. K. Kimura, S. I. Naya, Y. Jin-nouchi and H. Tada, *J. Phys. Chem. C*, 2012, **116**, 7111-7117.
10. M. J. Allen, V. C. Tung and R. B. Kaner, *Chem. Rev.*, 2010, **110**, 132-145.
11. A. K. Geim, *Science*, 2009, **324**, 1530.
12. M. D. Stoller, S. Park, Y. Zhu, J. An and R. S. Ruoff, *Nano Lett.*, 2008, **8**, 3498-3502.
13. H. I. Kim, G. H. Moon, D. Monllor-Satoca, Y. Park and W. Choi, *J. Phys. Chem. C*, 2012, **116**, 1535-1543.
14. T. Wang, C. H. Yang, C. L. Man, L. G. Wu, W. L. Xue, J. N. Shen, B. Van der Bruggen and Z. Yi, *Ind. Eng. Chem. Res*., 2017, **56**, 8981-8990.
15. Y. Zhang, Z. R. Tang, X. Fu and Y. J. Xu, *ACS Nano*, 2010, **4**, 7303-7314.
16. X. Jiang, X. Li, X. Jia, G. Li, X. Wang, G. Wang, Z. Li, L. Yang and B. Zhao, *J. Phys. Chem. C*, 2012, **116**, 14650-14655.
17. C. Liu, D. Yang, Y. Jiao, Y. Tian, Y. Wang and Z. Jiang, *ACS Appl. Mater. Interfaces*, 2013, **5**, 3824-3832.
18. B. Xin, L. Jing, Z. Ren, B. Wang and H. Fu, *J. Phys. Chem. B*, 2005, **109**, 2805-2809.
19. W. Gao, M. Wang, C. Ran, X. Yao, H. Yang, J. Liu, D. He and J. Bai, *Nanoscale*, 2014, **6**, 5498-5508.
20. Y. Wen, H. Ding and Y. Shan, *Nanoscale,* 2011, **3**, 4411-4417.
21. W. S. Hummers and R. E. Offeman, *J. Am. Chem. Soc.*, 1958, **80**, 1339-1339.
22. D. Guin, S. V. Manorama, J. N. L. Latha and S. Singh, *J. Phys. Chem. C*, 2007, **111**, 13393-13397.
23. J. S. Park, S. M. Cho, W. J. Kim, J. Park and P. J. Yoo, *ACS Appl. Mater. Interfaces*, 2011, **3**, 360-368.
24. N. T. McDevitt and W. L. Baun, *Spectrochim. Acta*, 1964, **20**, 799-808.
25. R. Liu, P. Wang, X. Wang, H. Yu and J. Yu, *J. Phys. Chem. C*, 2012, **116**, 17721-17728.
26. H. Yu, R. Liu, X. Wang, P. Wang and J. Yu, *Appl. Catal. B*, 2012, **111-112**, 326-333.
27. V. G. Pol, D. N. Srivastava, O. Palchik, V. Palchik, M. A. Slifkin, A. M. Weiss and A. Gedanken, *Langmuir*, 2002, **18**, 3352-3357.
28. Z. Zhang, F. Xiao, Y. Guo, S. Wang and Y. Liu, *ACS Appl. Mater. Interfaces*, 2013, **5**, 2227-2233.
29. A. Furube, L. Du, K. Hara, R. Katoh and M. Tachiya, *J. Am. Chem. Soc.*, 2007, **129**, 14852-14853.
30. H. Zhang, G. Wang, D. Chen, X. Lv and J. Li, *Chem. Mater.*, 2008, **20**, 6543-6549.